Arab J Sci Eng (2012) 37:291–301
DOI 10.1007/s13369-012-0172-y

RESEARCH ARTICLE - CIVIL ENGINEERING

F. B. A. Beshara · I. G. Shaaban · T. S. Mustafa

Nominal Flexural Strength of High Strength Fiber Reinforced Concrete Beams

Received: 26 May 2010 / Accepted: 24 April 2011 / Published online: 1 February 2012

Abstract This paper presents the development of simple semi-empirical formulae for the analysis of nominal flexural strength of high strength steel fiber reinforced concrete (HSFRC) beams. Such developed formulae were based on strain compatibility and equilibrium conditions for fully and partially HSFRC sections in joint with suitable idealized compression and tension stress blocks. The stress blocks were given by suitable empirical functions for the compressive and post-cracking strengths of HSFRC. The enhancement in compressive strength due to fibers inclusion is proposed as a function of concrete matrix strength and fiber reinforcing index. To account for the pullout resistance of fibers in tension, the post-cracking strength was evaluated as a function of fiber reinforcing index and bond strength. The fiber reinforcing index was considered as a function of volume content, aspect ratio, orientation and length efficiency factors of the fibers. In view of the degenerative nature of the pullout resistance of the fibers with the increase of crack width, a limit was placed on the useful tensile strain extent, depending on fiber length and crack spacing. It was found that there is a good agreement between the flexural strengths for HSFRC beams predicted by the proposed formulae and the experimental results reported in the literature, while the predicted flexural strengths as computed by ACI Committee 544.4R (ACI Struct J 85:563–580, 1988) and ACI Committee 544.1R (ACI Struct J 94:1–66, 1997) were very conservative. The parametric studies indicate that the nominal moment section capacity increases with the increase of fiber content and fiber aspect ratio.

Keywords Flexural strength · High strength concrete · Reinforced concrete beams · Steel fibers

الخلاصة

لتحقيق الفائدة المثلى للخرسانة عالية المقاومة – المستخدمة في مجالات عديدة مثل أعمدة المباني العالية و البحور الطويلة ؛ يتم إضافة ألياف الصلب اليها وذلك للتغلب على تقصفها وتحسين الممطولية. لذا يختص هذا البحث باستنباط طريقة جديدة لتصميم و تحليل الكمرات الخرسانية عالية المقاومة و المسلحة بأسياخ الصلب المعتادة و ألياف الصلب الموزعة عشوائيا المعروفة اختصارا (HSFRC) تحت عزوم الانحناء القصوى.

لقد تم تطوير المعادلات للتصميم والتحليل الانحنائى للكمرات باستخدام شروط الاتزان وتوافق الانفعالات للقطاعات مع توزيعات مستطيليه مكافئة لإجهادات الضغط و الشد القصوى ، وذلك عن طريق اشتقاق دوال نصف وضعية للقيم الحدية تأخذ تأثير المقاومة العالية للخرسانة و النسب الحجمية و البعدية و التوزيع العشوائي للألياف. كذلك تتناول الطريقة المقترحة تأثير آليات فقدان التماسك وسحب الألياف فى الشد عن طريق استخدام مقاومة الشد بعد التصدع التى يعبر عنها باستخدام علاقات نصف وضعية تعتمد على مقاومة التماسك ومؤشر التسليح بالألياف مع وضع حد مناسب للانفعال المفيد للخرسانة فى الشد الذى يعتمد على عرض الشرخ وطول الألياف. وقد تم استخدام الطريقة بنجاح لإجراء دراسات تأكيدية عديدة لنتائج البرامج التجريبية السابقة للكمرات ، وتبين أيضا أن النتائج النظرية لطريقة التصميم للكود الأمريكي متحفظة جداً لتلك الكمرات. وأخيراً تم إجراء دراسات بارامترية توضح أن مقاومة الانحناء القصوى لقطاعات HSFRC تزداد مع الزيادة الحجمية والبعدية للألياف.

F. B. A. Beshara (✉) · I. G. Shaaban · T. S. Mustafa
Faculty of Engineering at Shobra, Banha University, 108 Shobra St., Cairo, Egypt
E-mail: foush59@yahoo.com

1 Introduction

Nowadays, different structural applications such as beams, columns, and connections are being constructed using steel fiber reinforced concrete (SFRC) in combination with conventional steel reinforcing bars. When concrete cracks, the randomly oriented fibers arrest the internal micro-cracking mechanism and limit crack propagation, and in turn, improve strength and ductility under different loading schemes [3]. Several experimental programs have been worked out [4–6] to identify the flexural behavior of SFRC beams. It was found that SFRC beams exhibit higher flexural strength, ductility and toughness properties for longer fiber and higher fiber content. As shown in Figs. 1 and 2, the moment-deflection curve of SFRC beams has longer plateau at the peak load, and the descending part of curve is less steep compared to non-fibrous concrete beams.

The existing flexural design approaches for SFRC are based on conventional design methods supplemented by special procedures for fiber contribution [2,5]. Such methods are often empirical, and they may apply only to certain cases where limited supporting test data have been obtained. In [1,2], the flexural strength of SFRC sections is predicted on the basis of an equivalent rectangular compression and rectangular tension block. The compression block is defined in terms of the compressive strength of cylinder of concrete matrix while the tension block depends only on the bond strength of steel fibers (f_b). The bond strength is evaluated as 4.0 MPa. As shown in Fig. 3, the basic equations for calculating the nominal moment strength (M_n) are as follows:

$$M_n = T_s(d - a/2) + T_f(t/2 + c/2 - a/2) \tag{1}$$

$$T_f = f_b b(t - e) \tag{2}$$

The distance (e) is measured from extreme compression fiber to top of tensile stress block of fibrous concrete.

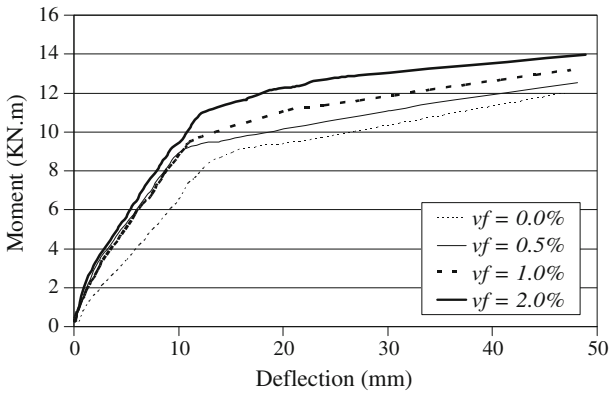

Fig. 1 Effect of steel fiber content on the load-deflection response [6]

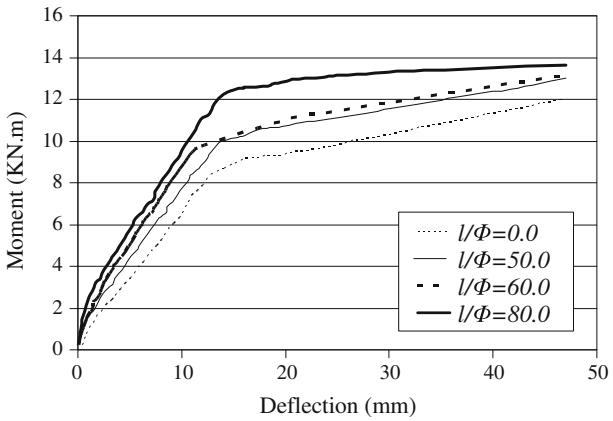

Fig. 2 Effect of steel fiber aspect ratio on the load-deflection response [6]

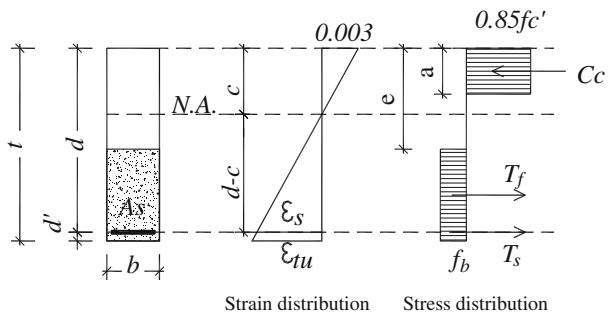

Fig. 3 ACI approach [1]

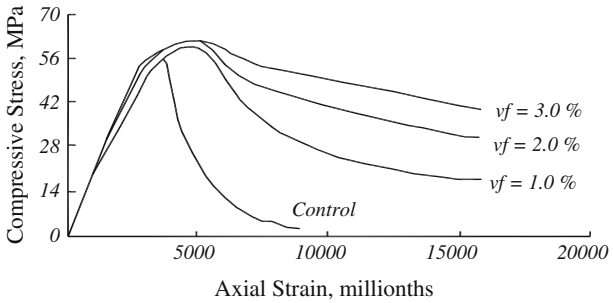

Fig. 4 Effect of fibers volume fraction on compressive stress-strain curves [2]

This paper presents a more realistic and semi-empirical approach for predicting the nominal flexural strength on the basis of suitable idealized stress blocks and sectional analysis procedure. The theoretical predictions of the ultimate moment capacity are compared with the measured response for many tested beams in other research programs mentioned in the literature.

2 Evaluation of HSFRC Parameters

To develop the proposed flexural strength state for HSFRC beams, the compressive strength and post-cracking strength of HSFRC are empirically evaluated.

2.1 Compressive Strength of HSFRC

Many experimental programs for SFRC under uni-axial compressive loading were worked out [1,7,8] to study the effect of steel fibers addition to normal and high strength concrete matrix. Typical stress-strain curves of SFRC in compression are given in Fig. 4 where the effect of increasing fiber content is shown to increase the area under the descending branch of the curve. The effect of increasing fiber aspect ratio follows the same trend as shown in Fig. 5. The main contribution of fibers inclusion is found to increase toughness, integrity and ductility of the composite in compression.

To evaluate the gain in compressive strength due to fibers inclusion in the present work, nine HSC cubes and eighteen HSFRC cubes with different fiber contents were tested after 28 days using the standard compression machine. The strength values for different concrete cubes are given in Table 1. It is clear that the compressive strength of the composite HSFRC has a slight increase than that of HSC matrix. This enhancement in uniaxial strength is due to the internal passive confinement of the matrix by steel fibers, which also delay the crack spreading and propagation [2].

To determine the strength gain of HSFRC, analytical expression was sought in terms of the fiber reinforcing parameters and compressive strength of HSC matrix. For this purpose, these key parameters were statistically related to the experimental data of HSFRC cubes. It was generally observed that the least square fitting linear relation was quite acceptable and simple. The following general form was used:

$$f_{\mathrm{cuf}} = f_{\mathrm{cu}}(a + bI_{\mathrm{f}}) \tag{3}$$

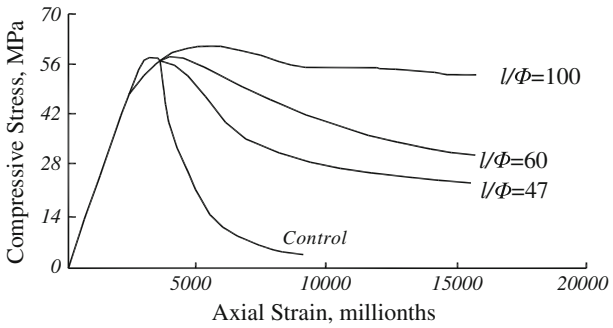

Fig. 5 Influence of fibers aspect ratio on compressive stress-strain curves [2]

Table 1 Summary of experimental results of standard cubes [6]

No. of cubes	Fiber volume (%)	Average strength (MPa)
9	0.0	80.3
6	0.5	81.5
6	1.0	84.3
6	2.0	89.65

where f_{cuf} and f_{cu} are, respectively, the compressive strength of HSFRC composite and HSC matrix. The constants a and b are the slope and intercept parameters of the linear fitting equation. In order to account for the random spatial distribution of discrete short steel fibers and for the fiber matrix interaction, the fiber reinforcing index If is considered as a function of fiber volume content v_f, fiber aspect ratio (l_f/Φ), orientation and length efficiency factors η_{oc}, η_{lc}

$$I_f = 2\eta_{lc}\eta_{oc}v_f(l_f/\Phi) \tag{4}$$

In the present work, fiber length was less than the critical fiber length and was much less than the dimension of cube specimen. In addition, the testing results of SFRC confirm the fact that steel fibers exhibited only pull-out mechanism at increasing strains. As a result, the values of η_{oc} and η_{lc} as 0.14 and 0.5 respectively have been applied in the present work for HSFRC in compression. The fiber reinforcing index If was given by:

$$I_f = 0.14v_f(l_f/\Phi) \tag{5}$$

From the statistical analysis of the experimental results [6], the following linear regression equation was derived to predict compressive strength of HSFRC composite as:

$$f_{cuf} = f_{cu}(1 + 0.1066v_f l_f/\Phi) \tag{6}$$

2.2 Post-cracking Strength of HSFRC

The existing studies on the tensile response of SFRC in literature [1,3,9], showed that the contribution of steel fibers to the brittle matrix can be simulated as: significant increase in material ductility and toughness, and steady state crack-width control mechanism. Typical example of the stress-crack width curve is shown in Fig. 6. It is clear that the stress-displacement curve consists of a small ascending part followed by long descending softening part.

After composite cracking, the load is transferred immediately to the fibers at the crack interface. Due to fibers debonding, the tensile stress response in the measured load-extension curves abruptly drops and is arrested at a certain level by the pullout resistance of fibers. This stress level is defined as the post-cracking strength f_{pp}. From the tension tests on fibrous concrete, the post-cracking strength is related [10] to the bond strength (τ_u), fiber volume content v_f, fiber aspect ratio (l_f/Φ), fiber length and orientation efficiency factors (η_{lt}, η_{ot}) in tension

$$f_{pp} = 2\eta_{lt}\eta_{ot}v_f(l_f/\Phi)\tau_u \tag{7}$$

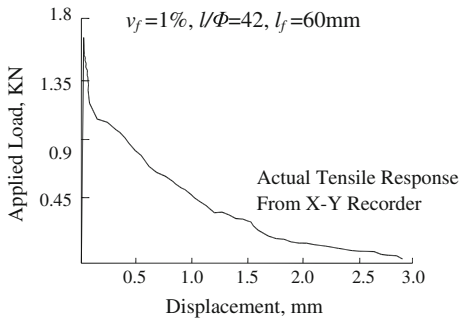

Fig. 6 Tensile load-displacement relationship of SFRC

For the present case when the fiber length was less than the dimensions of beam section, the values of η_{lt} and η_{ot} are 0.5 and 0.41 respectively. For the ultimate bond strength τ_u, a value of 4.0 MPa is adapted here [2]. The pullout resistance fpp, is given in MPa as

$$f_{pp} = 1.64 v_f (l_f/\Phi) \tag{8}$$

It was found [9,10] that the post-cracking stress drops approximately to zero at crack extension equal to half the fiber length.

3 Proposed Nominal Flexural Strength Approach for HSFRC Beams

Based on the strain compatibility & equilibrium conditions and suitable assumptions for HSFRC beam sections, the formulations of proposed approach are presented. According to ACI code [11], the ultimate moment strength (M_u) is as follows:

$$M_u = (\text{strength reduction factor}) * M_n \tag{9}$$

3.1 Basic Assumptions of the Approach

The proposed approach for flexure of HSFRC beams is based on the following assumptions:

- Plane sections remain plane after bending, and consequently the strain distribution is linear.
- The strain in the reinforcement is equal to the strain in concrete at the same level which implies perfect bond between concrete and steel.
- For steel reinforcement in compression and tension, the bilinear elasto-plastic idealization is used.
- For HSFRC in compression, the stress distribution is idealized by the equivalent rectangular stress block of ACI code [11]. A uniform stress of 0.67 f_{cuf} is assumed to be distributed over an equivalent compression zone of depth = a, given as a function of the neutral axis depth c.

$$a = \beta c \tag{10}$$

$$\beta = 1.05 - 0.05(f_{cuf}/6.9) \quad 0.85 \geq \beta \geq 0.65 \tag{11}$$

- Based on the study of plastic hinges, concrete is assumed to crush when the compression strain reaches a limiting usable strain which is taken as 0.003 [1]. It should be noted that much higher limiting strain have been measured in HSFRC members.
- Using a perfectly plastic idealization for the behavior of HSFRC in tension, the tensile stress rectangular distribution is represented by a uniform stress which equals the post-cracking strength f_{pp} and acting over a depth of $(t - c)$. The post-cracking strength accounts for the pullout resistance of steel fibers.

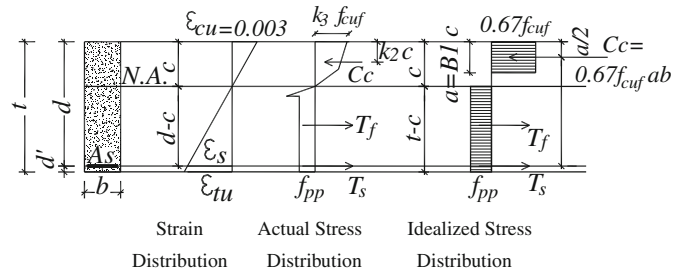

(a) *Fully Reinforced SFRC Section*

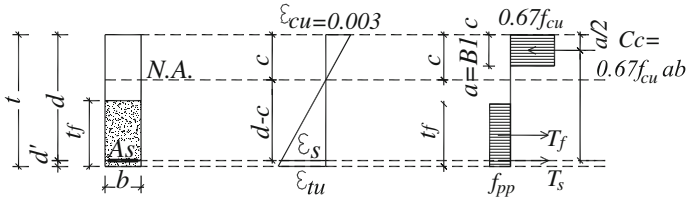

(b) *Partially Reinforced SFRC Section*

Fig. 7 Ultimate stress and strain distribution

- In view of the degenerative nature of the pullout resistance of steel fibers with the increase of crack width, a limit is placed on the useful tensile strain extent. Hence, ε_{tu} is set as a function of the fiber length l_f and the crack spacing S_{cr} [10].

$$\varepsilon_{tu} = l_f/8S_{cr} \tag{12}$$

Approximate value was evaluated for crack spacing as 0.5t to 0.8t [10,12].

- The compressive and post-cracking strengths of HSFRC are evaluated by the empirical functions given before.

3.2 Formulations of the Approach

Based on the above assumptions, the ultimate strain and stress distribution is shown in Fig. 7a for the fully reinforced HSFRC section, and in Fig. 7b for the partially reinforced HSFRC section; where the steel fiber is included only in the tension side over a depth of t_f, From the force equilibrium condition and strain compatibility condition, the depth of the compression block can be determined as follows:

$$C_c = T_s + T_f \tag{13}$$
$$T_s = A_s f_s \tag{14}$$
$$\varepsilon_s = 0.003(\beta d/a - 1) \tag{15}$$
$$f_s = E_s \quad \varepsilon_s \varepsilon_s < \varepsilon_y \tag{16}$$
$$f_s = f_y \quad \varepsilon_s \geq \varepsilon_y \tag{17}$$

For fully reinforced HSFRC section, the forces C_c and T_f are given by:

$$C_c = 0.67 f_{cuf} ab \tag{18}$$
$$T_f = 1.64 v_f (l_{f/}\Phi) b(t - c) \tag{19}$$

For the partially reinforced HSFRC section, the forces are given by:

$$C_c = 0.67 f_{cu} ab \tag{20}$$

$$T_f = 1.64 v_f (l_f/\Phi) b t_f \tag{21}$$

From the equilibrium condition of moments, the nominal moment capacity of the fully reinforced HSFRC section is expressed by:

$$M_n = T_s(d - \beta c/2) + T_f[(t + c - \beta c)/2] \tag{22}$$

The corresponding nominal moment capacity of partially reinforced HSFRC section is:

$$M_n = T_s(d - \beta c/2) + T_f[t - (t_f + \beta c)/2]. \tag{23}$$

4 Validation and Parametric Studies

4.1 Verification Studies

Using the proposed approach, the nominal moments of several SFRC beams are computed and compared with the experimental results from eight sources of literature. In Table 2, the predicted moments are compared with the testing results for 39 beams. In addition, the examinations of all tested and computed strengths are shown in Fig. 8. The study of the results listed in the table and the figure showed that satisfactory results were obtained from the comparison of measured and computed flexural strengths. The mean value of the ratio between the measured and calculated strengths is 1.17 and the standard deviation is 0.09. The approach yields safe predictions for nominal moment capacity for normal strength and high strength fibrous concrete beams.

Despite the difference in test specimens, Table 2 and Fig. 8 show that the proposed approach predicts the flexural strength of test specimens reasonably well. Data cover a broad spectrum of fibrous beams including variations in concrete strength ($34 \leq f_{cuf} \leq 90$ MPa), steel yield stress ($360 \leq f_y \leq 437$ MPa), tensile steel area ($25 \leq A_s \leq 628\,\text{mm}^2$), compression steel area ($0 \leq A_s' \leq 100\,\text{mm}^2$), beam widths ($110 \leq b \leq 250$ mm), beam depth ($100 \leq t \leq 300$ mm), fiber volume content ($0.0 \leq v_f \leq 2.0\%$), fiber aspect ratio ($30 \leq l_f/\Phi \leq 80$), and fiber zoning (Full, Partial). Moreover, Table 2 shows that the ultimate moment capacity for fibrous beams increases with the increase of concrete strength, yield stress of steel, tension steel ratio, and compression steel ratio. The tensile strain was monitored at the extreme tension side and the computed values were in the range of 0.006–0.05. These values have not exceeded the tensile strain limit as given by Eq. (12); $\varepsilon_{tu} = l_f/4t$.

In Table 2, the flexural strengths of the different experimental results of fibrous beams are recalculated using ACI equations. In addition, the examinations of all tested and computed strengths are shown in Fig. 9. The mean value of the ratio between the measured and calculated strengths is 1.50 and the standard deviation is 0.30. The study of the results listed in the table and the figure showed that ACI predictions of nominal moment capacity of SFRC sections are very conservative in comparison with the proposed method.

4.2 Parametric and Design Studies

Several case studies were performed to demonstrate the variation in the calculated flexural strength of HSFRC beams caused by the fiber reinforcing parameters. The beam with $v_f = 1.0\%$, tested in [6], was taken as the datum beam for the parametric design studies. The effect of fiber volume content, fiber aspect ratio, and fiber zoning on the nominal moment is shown in Fig. 10. The study of the results in this figure indicate that for constant fiber aspect ratio =50, the increase of v_f from 0.0 to 2.0% increases the moment capacity by 30.0% for fully reinforced HSFRC beam. For the case $l_f/\Phi = 80$, the corresponding increase in flexural strength is 47.0%. It can also be seen from Fig. 10 that the increase of fiber aspect ratio l_f/Φ from 50 to 80 leads to 7.7% increase in flexure strength if $v_f = 1.0\%$, and to 13.5% increase in flexure strength if $v_f = 2.0\%$. In addition, the

Table 2 Comparison between experimental results and predictions of design equations

Reference	Input data							M_{nexp} (KN.m)	Predicted		ACI	
	b × t (mm)	A_s (mm^2)	A'_s (mm^2)	f_y (MPa)	v_{sf} (%)	l_f/Φ	f_{cu} (MPa)		M_{np} (KN.m)	M_{nexp}/M_{np}	M_{nACI} (KN.m)	M_{nexp}/M_{nACI}
[6]	120 × 175	157	100	360	0.00	––	80.4	11.85	10.86	1.09	8.28	1.43
[6]	120 × 175	157	100	360	0.50	50	81.6	12.97	11.18	1.16	8.28	1.56
[6]	120 × 175	157	100	360	1.0	50	84.4	13.52	11.68	1.16	8.29	1.63
[6]	120 × 175	157	100	360	2.0	50	89.6	14.36	12.93	1.11	8.30	1.73
[6]	120 × 175	157	100	360	1.0	60	84.4	13.62	11.68	1.17	8.29	1.64
[6]	120 × 175	157	100	360	1.0	80	84.4	14.02	11.68	1.20	8.29	1.69
[6]	120 × 175	157	100	360	0.50	50	81.6	12.19	10.89	1.12	8.29	1.47
[6]	120 × 175	157	100	360	1.0	50	84.4	12.87	11.10	1.16	8.29	1.55
[6]	120 × 175	157	100	360	2.0	50	89.6	13.65	11.82	1.15	8.30	1.64
[6]	120 × 175	157	100	360	1.0	50	84.4	13.60	11.10	1.17	8.29	1.57
[6]	120 × 175	157	100	360	1.0	50	84.4	13.69	11.10	1.18	8.29	1.58
[13]	100 × 150	157	–	412	0.75	75	85	9.6	8.78	1.09	7.8	1.23
[13]	100 × 150	157	–	412	1.50	75	85	10.95	9.72	1.13	7.8	1.40
[10]	100 × 100	157	–	420	0.50	30	80	4.85	4.65	1.04	4.54	1.07
[10]	100 × 100	157	–	420	1.0	50	80	5.0	4.75	1.05	4.54	1.10
[10]	100 × 100	157	–	420	1.50	30	80	5.40	4.84	1.12	4.54	1.17
[14]	100 × 125	157	56.5	400	0.50	50	42	6.87	6.10	1.13	5.87	1.17
[14]	100 × 125	157	56.5	400	1.0	50	42	7.19	6.34	1.13	5.89	1.22
[14]	100 × 125	157	56.5	400	1.50	50	42	7.22	6.54	1.10	5.88	1.23
[14]	100 × 125	157	56.5	400	2.0	50	42	7.51	6.71	1.12	5.87	1.28
[15]	250 × 250	400	–	470	0.50	75	35	61.2	44.38	1.38	39.91	1.53
[15]	250 × 250	400	–	470	1.0	75	35	63	48.40	1.30	39.89	1.58
[15]	250 × 250	400	–	470	1.50	75	35	64.8	52.01	1.25	39.85	1.63
[15]	250 × 250	400	–	470	1.0	60	35	60	46.75	1.28	39.85	1.51
[16]	170 × 300	628	–	437	0.50	75	87	116.5	90.69	1.28	69.73	1.67
[16]	170 × 300	628	–	437	1.0	75	88	122.8	95.41	1.29	69.77	1.76
[16]	170 × 300	628	–	437	1.5	75	90	130.4	100.4	1.29	69.85	1.87
[16]	170 × 300	628	–	437	0.50	75	87	115.7	90.69	1.27	69.73	1.66
[16]	170 × 300	628	–	437	1.0	75	88	118.5	95.41	1.24	69.77	1.70
[16]	170 × 300	628	–	437	1.5	75	90	120.8	100.4	1.20	69.85	1.73
[17]	100 × 140	25	–	412	1.20	60	46	3.12	2.51	1.24	1.24	2.52
[17]	100 × 140	25	–	412	0.89	75	42	2.90	2.45	1.18	1.24	2.34
[17]	100 × 140	305	–	412	1.20	60	46	17.40	13.60	1.28	13.06	1.33
[17]	100 × 140	305	–	412	0.89	75	42	17.27	13.31	1.30	12.84	1.35
[18]	175 × 375	988	–	412	1.75	55	34	169.5	137.26	1.23	126	1.35
[18]	175 × 375	988	–	412	1.75	55	41	135.6	133	1.02	128.83	1.05
[18]	175 × 375	988	–	412	1.75	45	35	138.9	136	1.02	126.5	1.09
[18]	175 × 375	988	–	412	1.75	55	39	192.1	140.92	1.36	128.13	1.50
[18]	175 × 375	988	–	412	1.75	55	70	155.6	152.77	1.02	134.45	1.15
Overall average										1.17		1.50
Overall standard deviation										0.09		0.30

predicted flexural strength for partially reinforced HSFRC beams is slightly less than that of fully reinforced HSFRC beams.

To develop a flexural design chart for fully reinforced HSFRC sections, the governing equilibrium equations are rearranged and the following dimensionless formula was derived for all grades of concrete and steel and with different fiber reinforcing index.

$$M_n/(bd^2 f_{cuf}) = \mu(f_y/f_{cuf})(1 - \beta c/2d) + (f_{pp}/f_{cuf})\,[(t - c)/d]\,[(t + c - \beta c)/2d] \tag{24}$$

The design chart is plotted in Fig. 11. It is clear that the nominal moment capacity for a given section increases with the increase of longitudinal steel ratio (μ) or with the increase of fiber reinforcing index (I_f).

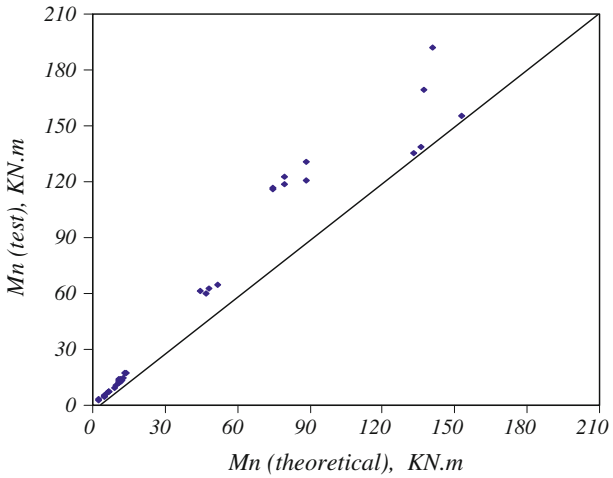

Fig. 8 Correlation of the experimental and design flexural strengths for the proposed method

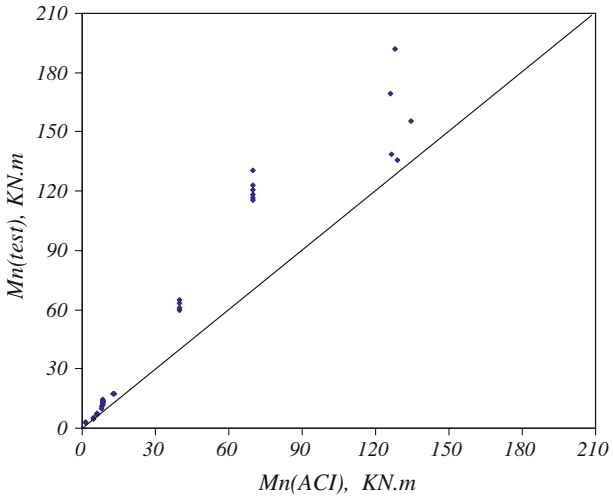

Fig. 9 Correlation of the experimental and design flexural strengths for the ACI equations

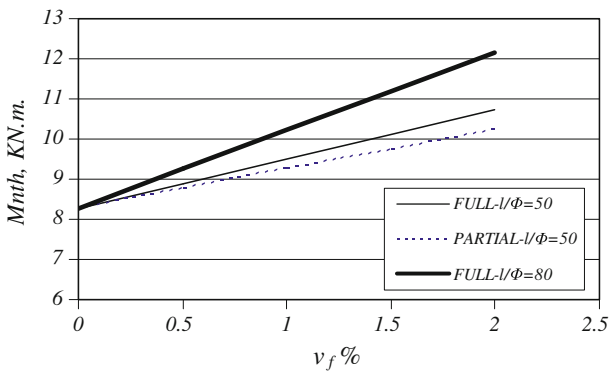

Fig. 10 Effect of fiber volume, aspect ratio, and fiber zoning on the predicted nominal moment

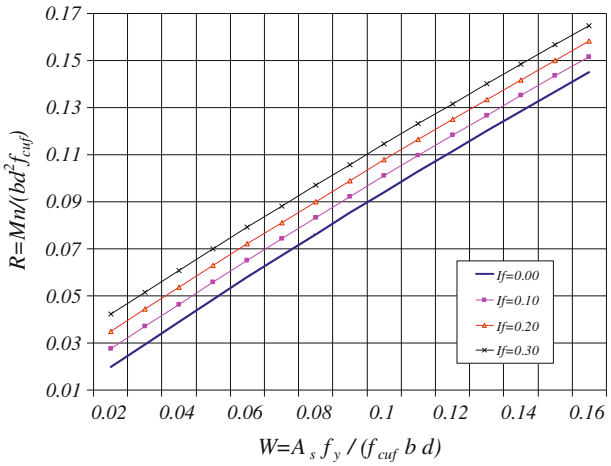

Fig. 11 Design chart for all grades of concrete and steel with different fiber reinforcing indices If

5 Conclusions

There is a good agreement between the computed flexural strengths by the proposed ultimate strength state for HSFRC beams, and the experimental results of several sources of literature. Despite the difference in test specimens, concrete strength, reinforcement details, and fiber parameters, the proposed approach predicts the flexural strength reasonably well and proves the suitability as a design and analysis tool. The mean value of the ratio between the measured and calculated strengths is 1.17 and the standard deviation is 0.09. The predicted flexural strengths as computed by [1] are very conservative where the mean value of the ratio between the measured and calculated strengths is 1.50 and the standard deviation is 0.30. The sensitivity studies of the governing fiber parameters indicate that the nominal moment capacity for a given HSFRC section increases with the increase of fiber volume fraction and fiber aspect ratio. For different fiber contents, the predicted flexural strengths for partially reinforced SFRC beams are slightly less than that of fully reinforced SFRC beams. Furthermore, the validation studies indicate the increase of nominal moment capacity with the increase of concrete strength, yield stress of steel, tension steel ratio, and compression steel ratio.

References

1. ACI Committee 544.4R: Design considerations for steel fiber reinforced concrete. ACI Struct. J. **85**, 563–580 (1988) (Reapproved 2002)
2. ACI committee 544.1R: State-of-the-art report on fiber reinforced concrete. ACI Struct. J. **94**, 1–66 (1997) (Reapproved 2002)
3. Shah, S.P.; Baton, G.B.: Fiber reinforced concrete: properties and applications. ACI, **SP-105** (1989)
4. Daniel, L.; Loukili, A.: Behavior of high strength fiber reinforced concrete beams under cyclic loading. ACI Struct. J. **99**, 248–256 (2002)
5. Altun, F.; Haktanir, T.; Ari, K.: Experimental investigation of steel fiber reinforced concrete box beams under flexure. Mater. Struct. **39**, 491–499 (2006)
6. Mustafa, T.S.: Behavior of High Strength Fiber Reinforced Concrete Beams. M.Sc thesis, Banha University (Faculty of Engineering) (2007)
7. Balaguru, P.N.; Shah, S.P.: Fiber Reinforced Cement Composites. Mc Graw Hill, Inc., New York (1992)
8. Balaguru, P.; Ramesh, N.; Mahendra, P.: Flexural toughness of steel fiber reinforced concrete. ACI Mater. J. **89**, 541–546 (1992)
9. Barros, J.A.; Cunha, V.M.; Antunes, J.A.: Postcracking behavior of steel fiber reinforced concrete. Mater. Struct. **38**, 47–56 (2005)
10. Lim, T.Y.; Paramasivam, P.; Lee, S.L.: Bending behavior of steel fiber concrete beams. ACI Struct. J. **84**, 524–536 (1987)
11. ACI Committee 318: Building Code Requirements for Structural Concrete (ACI 318M-05) and Commentary (ACI 318-R-99). ACI, Detroit (2005)
12. Laura, C.: Cracking of reinforced concrete elements. Oviduis Univ. Ann. Ser. **1**, 37–44 (2007)
13. Ashour, S.A.; Wafa, F.F.: Flexural behavior of high-strength fiber reinforced concrete beams. ACI Struct. J. **90**, 279–287 (1997)
14. Tan, K.H.; Paramasivam, P.; Tan, K.C.: Instantaneous and long term deflections of steel fiber reinforced concrete beams. ACI Struct. J. **91**, 384–393 (1994)
15. Al Sayed, S.H.: Flexural deflection of reinforced fibrous concrete beams. ACI Struct. J. **90**, 72–76 (1993)

16. Ashour, S.A.; Mahmood, K.; Wafa, F.F.: Influence of steel fibers and compression reinforcement on deflection of high strength concrete beams. ACI Struct. J. **94**, 611–624 (1997)
17. Kormeling, H.A.; Reinhadt, H.W.; Shah, S.P.: Static and fatigue properties of concrete beams reinforced with bars and fibers. ACI J. **77**, 36–43 (1980)
18. Craig, R.: Flexural behavior and design of reinforced fiber concrete members. Fiber Reinf. Concr. Prop. Appl. **SP-105**, 517–564 (1987)